

Validation of the hadronic calibration of the ATLAS calorimeter with testbeam data corresponding to the pseudorapidity range $2.5 < |\eta| < 4.0$

Gennady Pospelov
MPI Munich

*on behalf of ATLAS local hadronic calibration group
and the ATLAS liquid argon EMEC/HEC/FCAL collaboration*

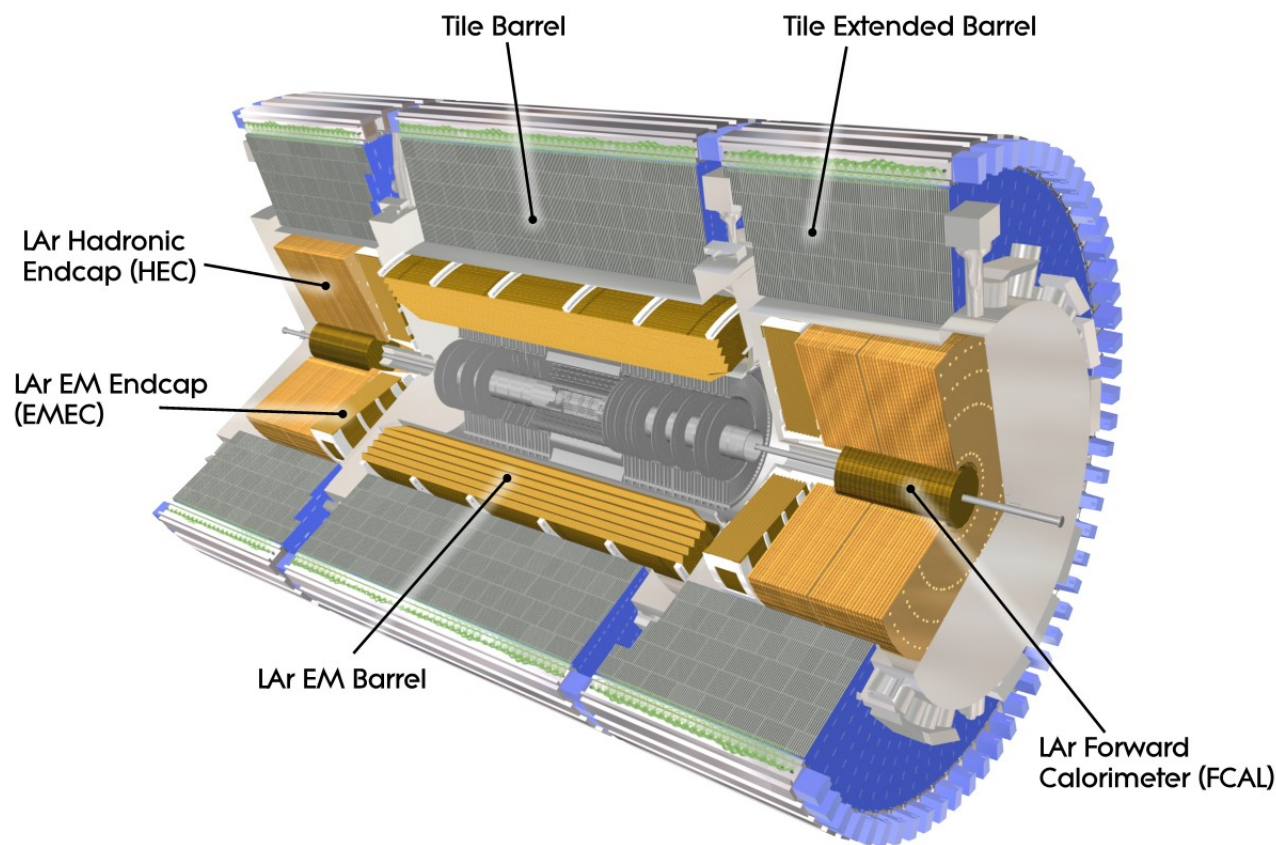
ICATPP09 Conference

Villa Olmo, Como, Italy, 5-9 October 2009

Outline

- Pions in the ATLAS calorimeter
- Local hadronic calibration schema
- Performance example for single pions in ATLAS simulations
- Setup for combined testbeam of LAr detectors in the forward region
- Measured Data & MC description
- Data/MC comparison for basic cluster quantities
- Basic performance for pions
- Conclusion

ATLAS calorimeters



Electromagnetic calorimeters:

acceptance $|\eta| < 3.2$
 depth $\sim 22X_0$
 number of channels 173952
 cluster noise 250 MeV
 design goals

$$\frac{\sigma(E)}{E} = \frac{10\%}{\sqrt{E}} \oplus \frac{0.3}{E} \oplus 0.7\%, \quad E \text{ in GeV}$$

nonlinearity $< 0.1\%$

Hadron and forward calorimeters:

acceptance $|\eta| < 5.0$
 number of channels 19000
 absorption length $9.7 - 13 \lambda$
 design goal for jets

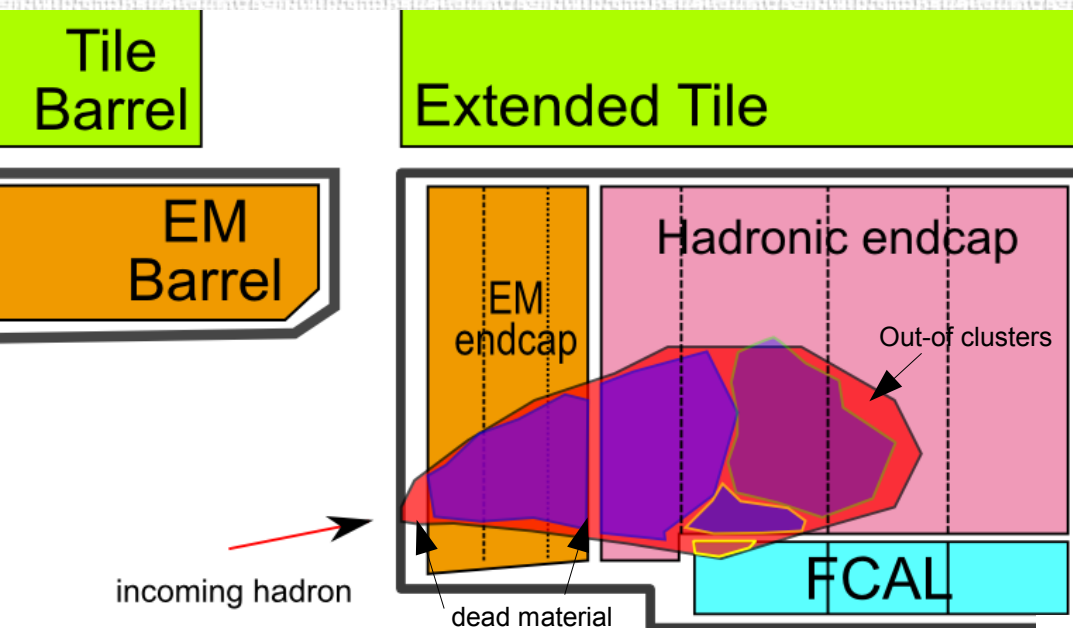
$$\frac{\sigma(E)}{E} = \frac{50\%}{\sqrt{E}} \oplus 3\%, \quad |\eta| < 3$$

$$\frac{\sigma(E)}{E} = \frac{100\%}{\sqrt{E}} \oplus 5\%, \quad 3 < |\eta| < 5$$

nonlinearity $< 2\%$

- The jet energy scale is the major source of uncertainty for measurements of the top quark mass and inclusive jet cross sections

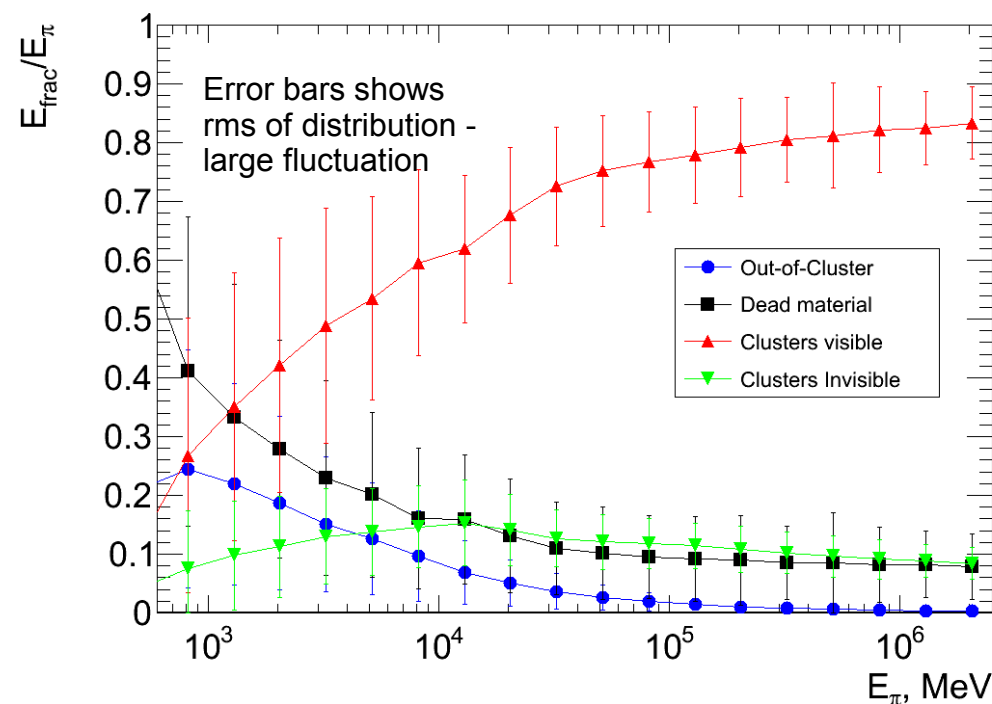
Pion in ATLAS calorimeter



- Factors responsible for nonlinearity and resolution degradation of hadrons
 - $e/h > 1$ for each calorimeter system (invisible energy)
 - energy in non-instrumented regions
 - energy outside of any reconstructed calorimeter objects (clusters)

- For 10 GeV pions at $\eta \sim 2.5$
 - $O(60\%)$ - energy in reconstructed clusters
 - $O(15\%)$ - invisible energy in clusters
 - $O(15\%)$ - energy in dead material
 - $O(10\%)$ - out-of-cluster energy
 - contributions depend on pion energy and are the subject of large fluctuations (see right-hand plot)

Calibration techniques are used to recover linearity and improve resolution.



Local hadronic calibration schema

- Calibration of topological clusters to particle level
 - Based on single pion simulations & GEANT4 truth energy deposits

3-d topological clusters with cells at e.m. scale.

classify clusters as e.m., had. or Unknown

cluster calibration

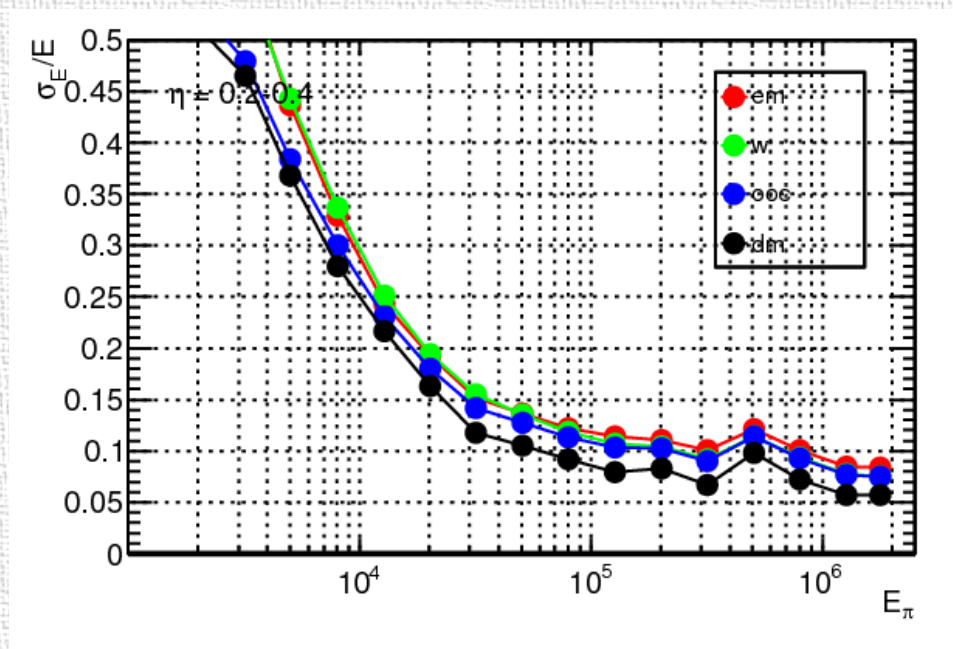
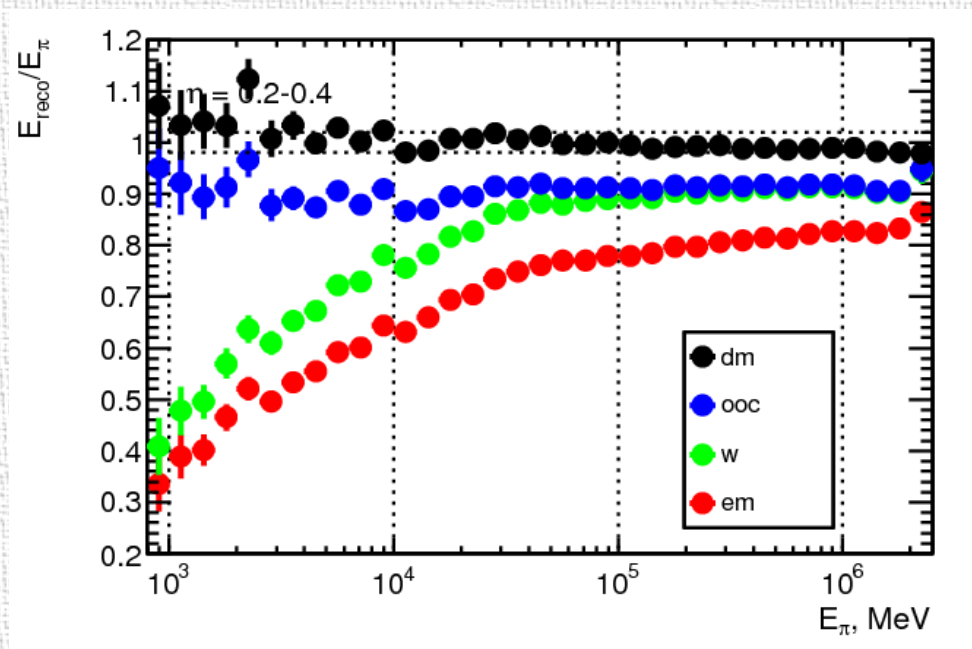
out-of-cluster correction

dead material correction

calibrated clusters

- Cluster making starts from calorimeter cells at e.m. scale
 - Starting from seed $|E_{\text{cell}}| > 4\eta_{\text{noise}}$, expanding in 3D around neighbors with $|E_{\text{cell}}| > 2\eta_{\text{noise}}$, finally adding perimeter cells $|E_{\text{cell}}| > 0$, split clusters around local maxima
- Classification to identify e.m. and non-e.m. parts of the shower
 - High average cell energy density $\langle \rho_{\text{cell}} \rangle$ and small cluster depth λ_{center} denote e.m. nature of cluster
- H1-style cells weighting for clusters classified as hadronic to account for non-compensation of the calorimeter
- Correction for energy deposited in calorimeter cells outside of any clusters due to noise thresholds
- Recovers lost energy in dead material in front and between calorimeter modules
- Clusters are calibrated to the particle level
 - Provides different jet algorithms with single input
 - Factorization of different effects

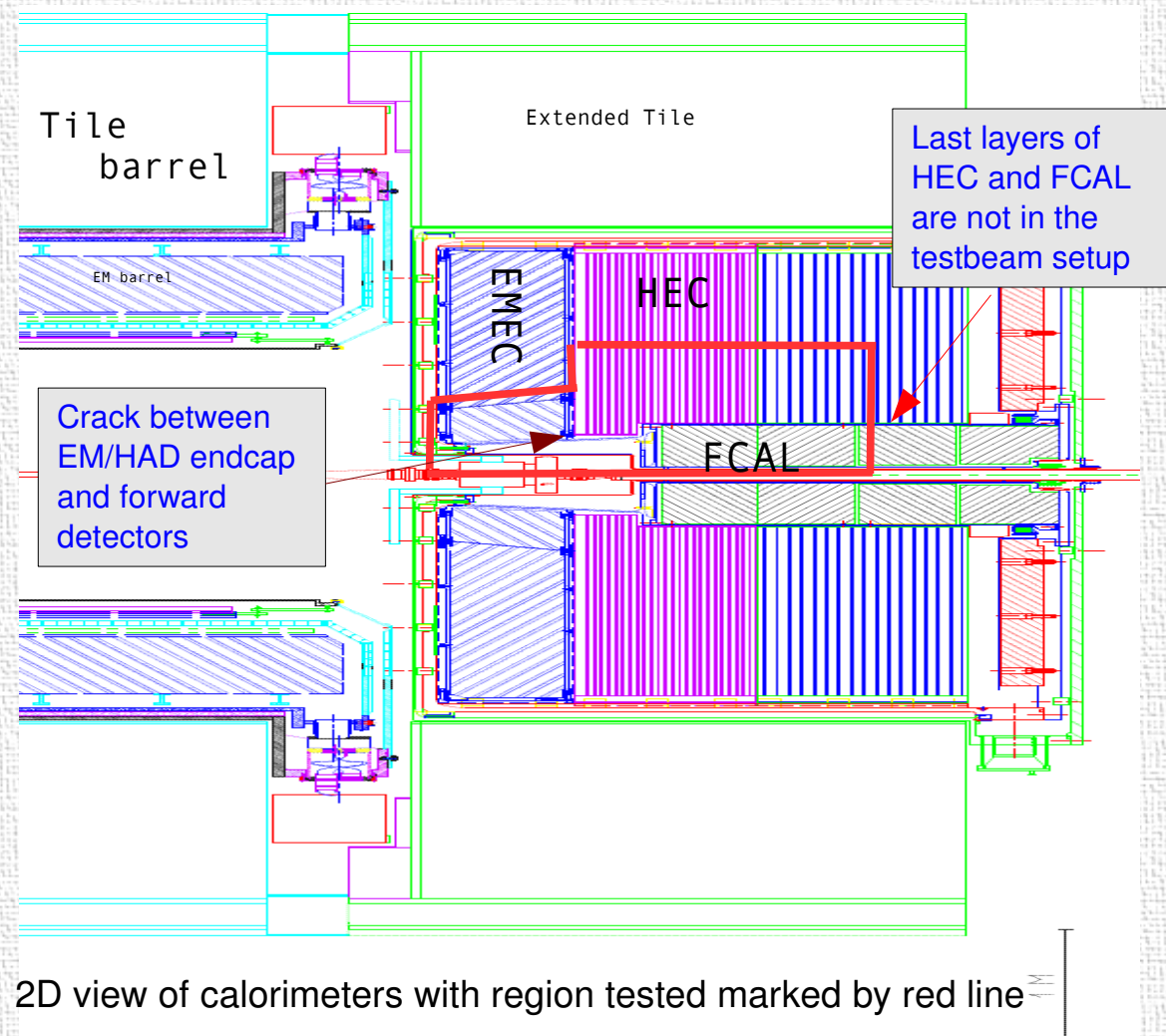
Single pion performance in ATLAS (Monte-Carlo)



- Reconstructed pion energy (left) and energy resolution (right) as a function of initial pion energy after each step of local hadronic calibration
 - Each step of calibration improves linearity and resolution
 - After the last step (dead material correction) relative resolution was improved by ~30%, linearity is recovered within $\pm 2\%$

Combined testbeam of LAr detectors in the forward region

- Combined test in 2004 of three LAr detectors in ATLAS forward region closed extensive program of beam tests started in 1996
 - NIM A 593 (2008) 323-342 describes performance for electrons/pions at e.m. scale
 - Subject of this talk – validation of ATLAS calorimeter reconstruction software (local hadronic calibration)
- One quadrant (module 0) of EMEC Inner Wheel
 - LAr + lead, accordion shape, 1/8 of whole wheel
 - Readout segmentation 0.1×0.1 ($\Delta\eta \times \Delta\phi$)
- One quadrant in phi of HEC
 - LAr + parallel flat copper plates
 - Readout segmentation 0.1×0.1 ($\Delta\eta \times \Delta\phi$) in outer, 0.2×0.2 in inner wheel
- One quadrant in phi of FCAL
 - LAr, EM part copper, HAD part tungsten alloy
 - Cylindrical electrodes parallel to the beam
 - Readout segmentation not projective, $\sim 0.2 \times 0.2$
- Dead material between calorimeter and in front of FCAL as close as possible to nominal ATLAS situation.

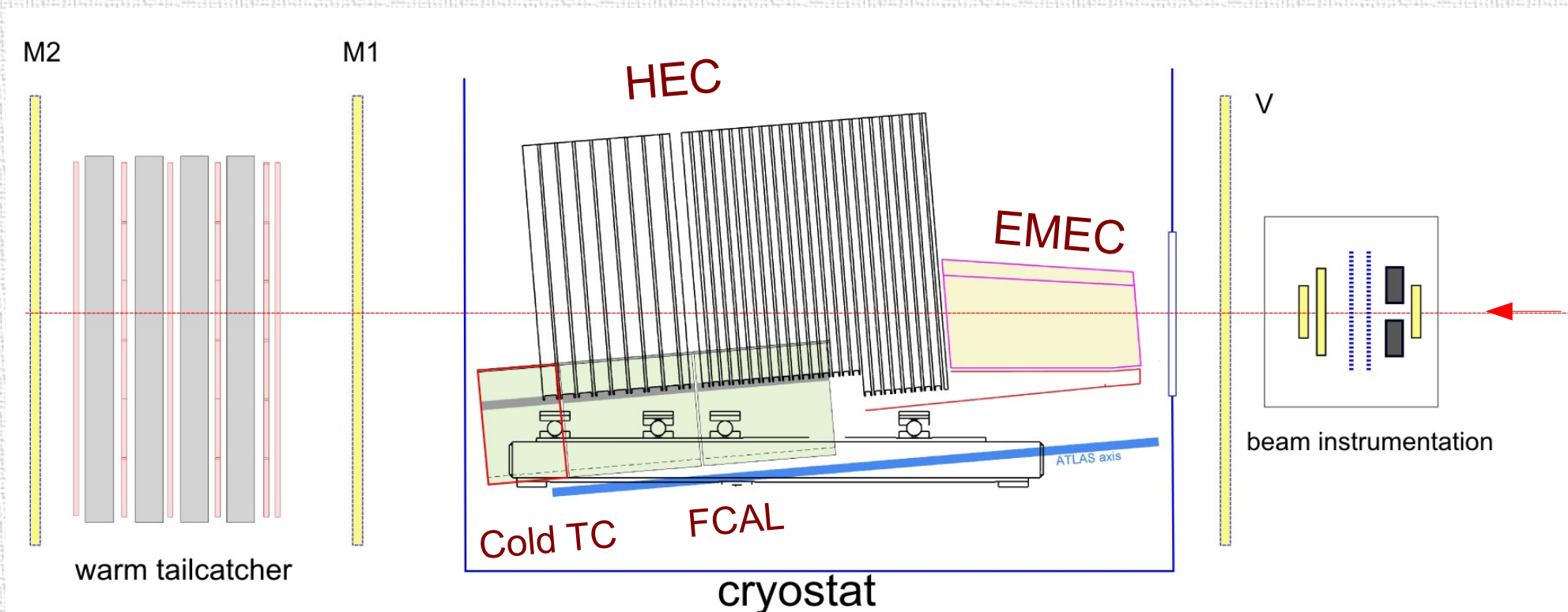


Setup

- Setup placed in H1 cryostat in CERN North Hall, using the H6 beam line
 - Limited acceptance because of space constraint in H1 cryostat
 - The setup is tilted to be projective at $\eta=2.8$

Experimental setup includes

- Beam instrumentation: multiwire proportional chambers, scintillation counters, scintillation walls
- Cryostat with EMEC, HEC and FCAL calorimeter modules
- Warm and cold tail catchers to help identify longitudinal leakage



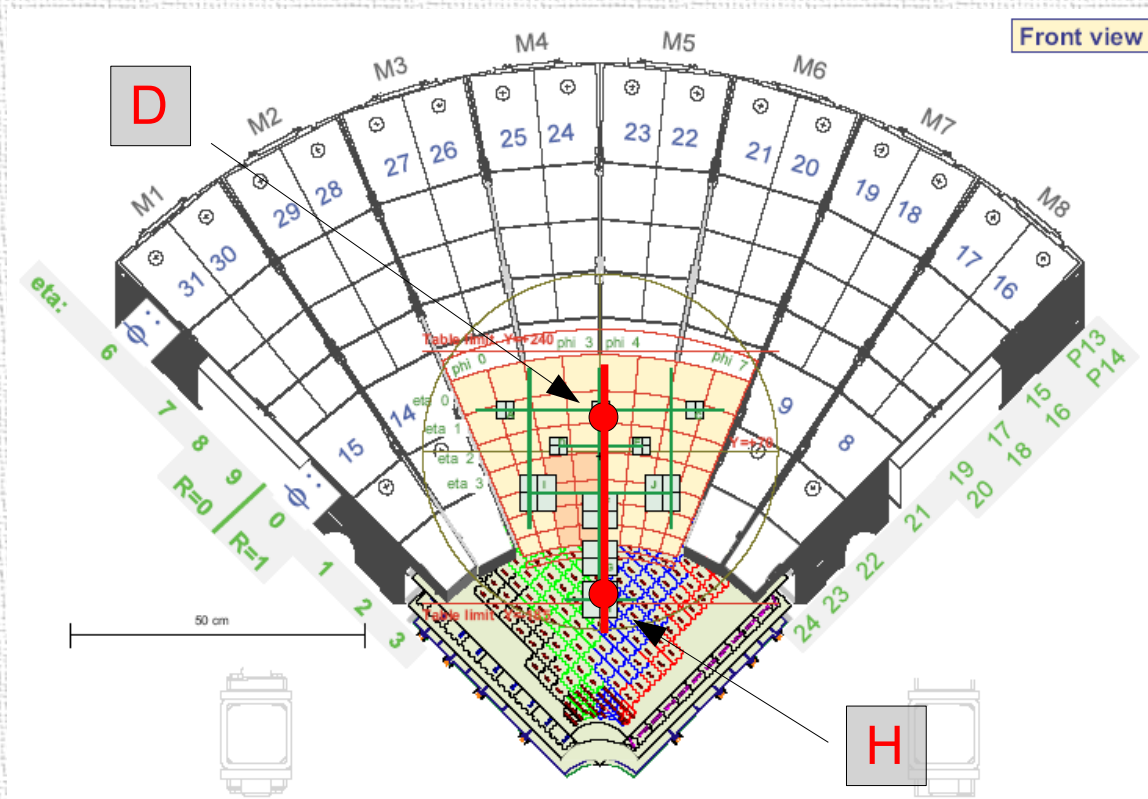
Data and Monte-Carlo

Data

- Various energy and position scans were performed for e^-,π in the energy range $6\text{GeV} < E < 200\text{GeV}$ with about 80 million triggers in total
 - Energy scans at a standard set of impact point (e.g. impact point **D** for the endcap area corresponding to $\eta=2.8$, impact point **H** for the forward area corresponding to $\eta=3.65$)
 - Position **X,Y** scans to cover full crack region

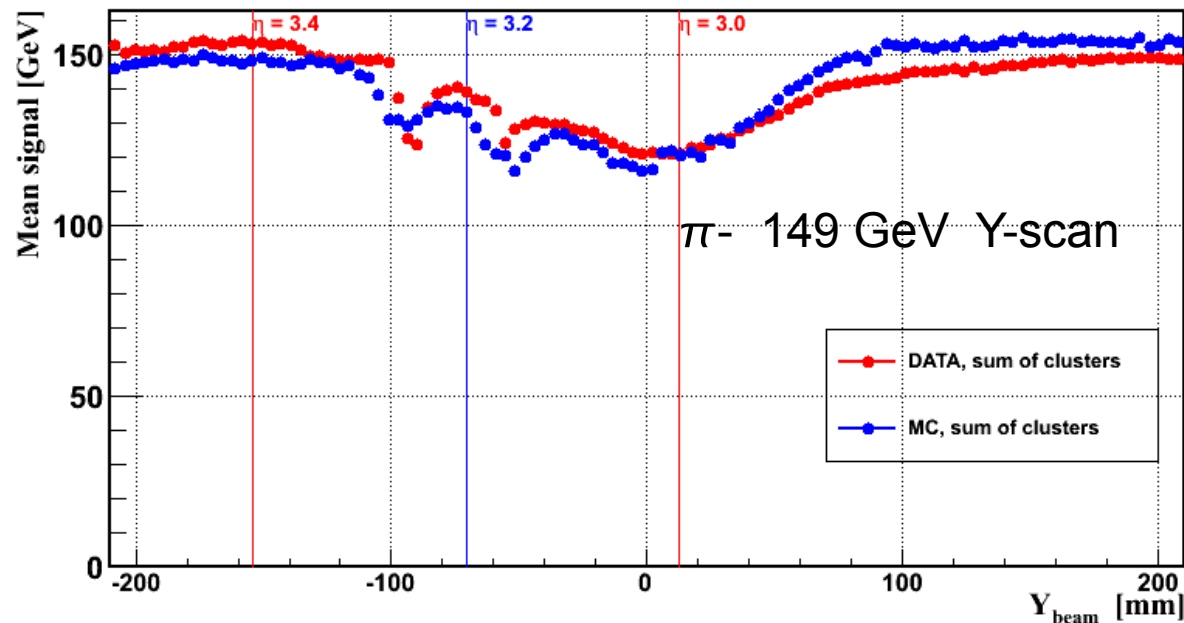
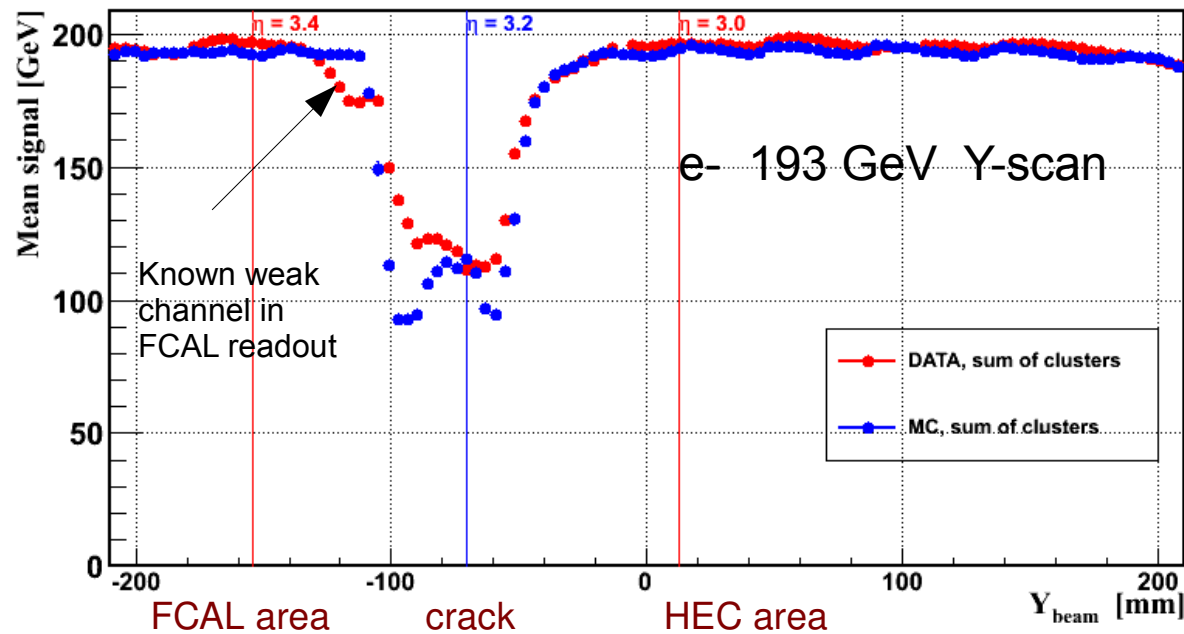
Monte-Carlo simulation

- Geant4 9.2.p00 with consistent description of testbeam setup
 - Range cut $30\text{ }\mu\text{m}$
 - QGSP_BERT physics list
- Reconstruction with ATLAS software release 15.3.0
 - hadronic calibration constants are corresponding to ATLAS geometry and not yet testbeam specific



Front view of the setup showing different beam impact points

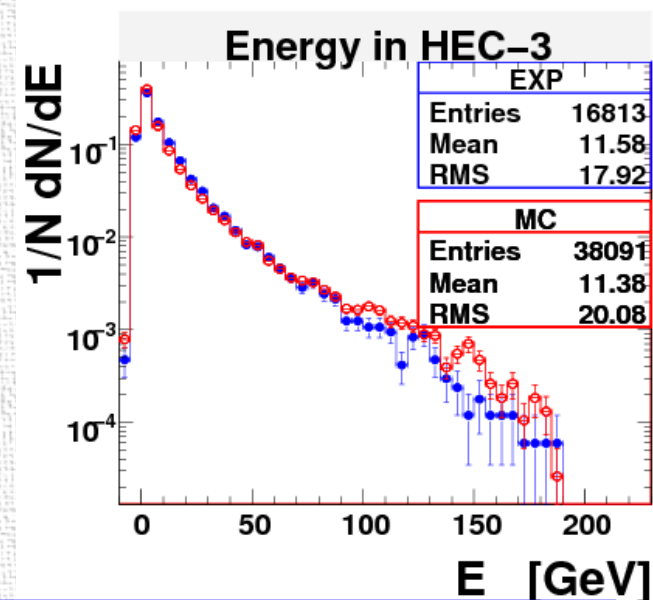
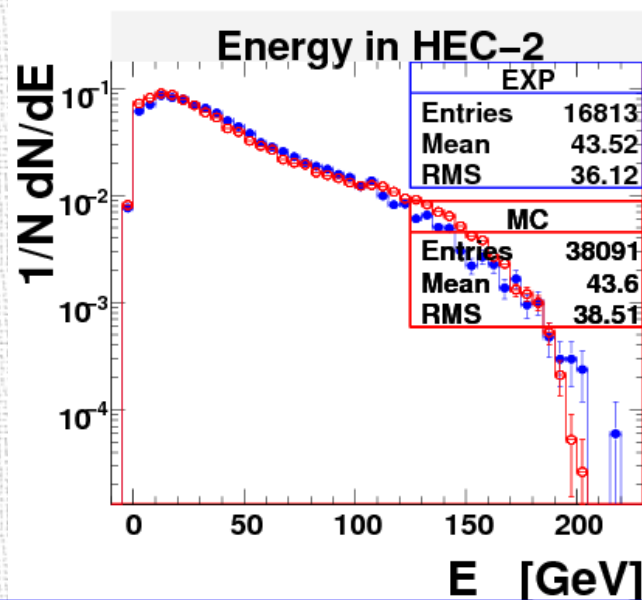
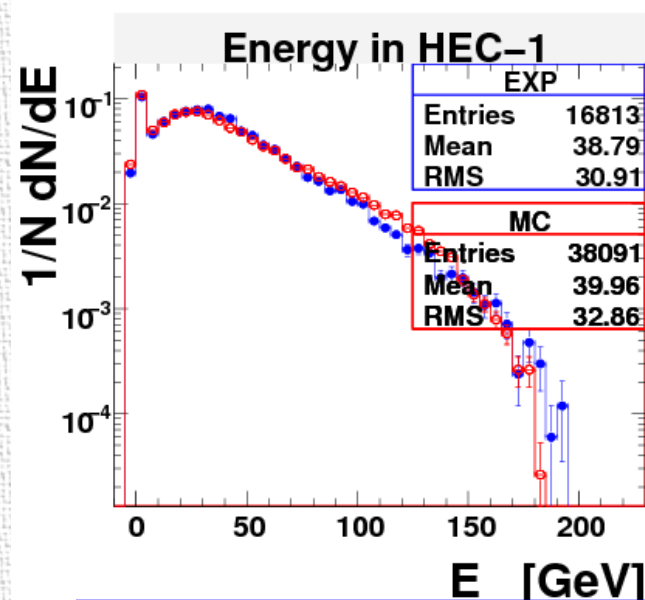
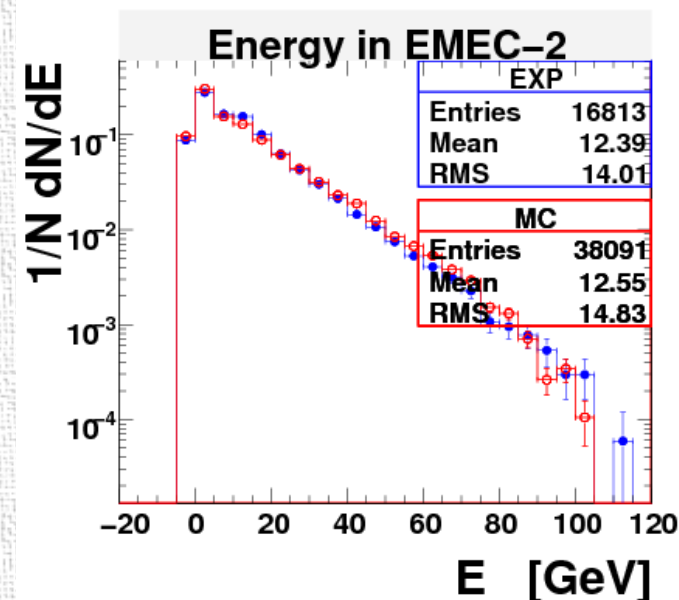
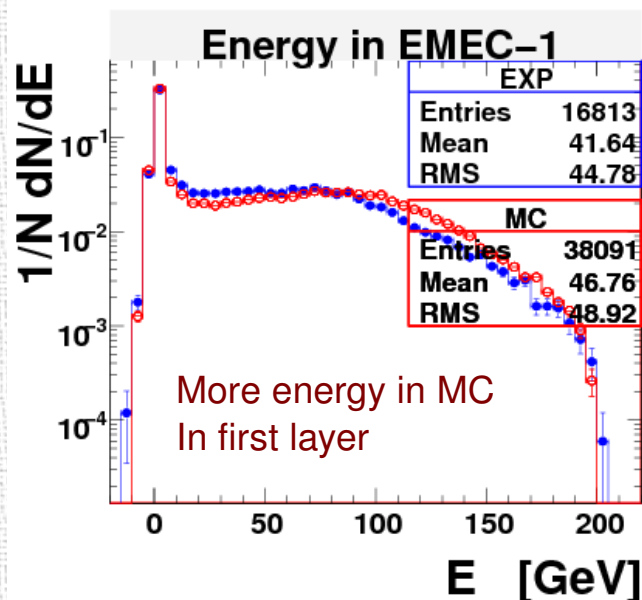
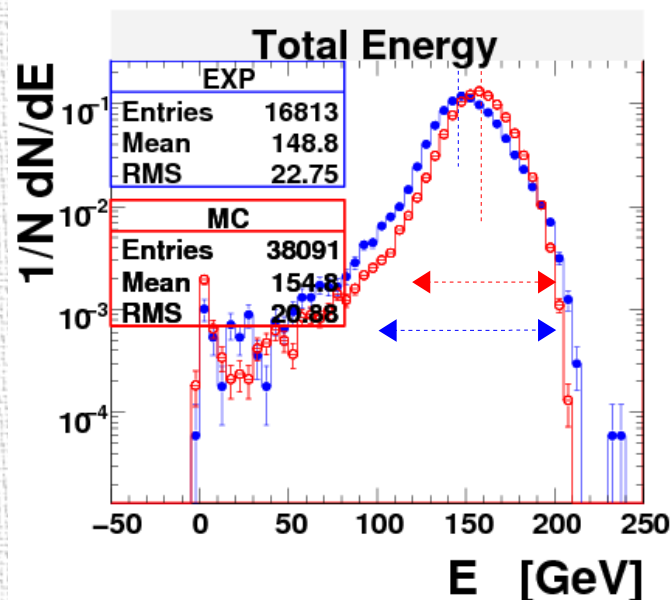
Vertical scan with electrons and pions



- Dependence of mean signal response at em-level on the beam position across endcap-forward region crack
 - Good check of MC geometry
- Electron scan (top plot)
 - Energy response quite nicely described outside crack (good em scale)
 - some discrepancy inside the crack (indication of clustering peculiarities there)
- Pion scan (bottom plot)
 - There are differences in MC versus DATA response – In forward region MC response is 3% lower, in endcap area it is 4% higher than in DATA
 - This is a QGSP_BERT issue

Energy in calorimeters in the endcap region (point D)

200 GeV pions at e.m. scale



Monte-Carlo in comparison to the data: total energy deposited is larger, distribution is narrower.
More energy deposited in the first layer (EMEC-1) –hint that earlier showering in MC is present

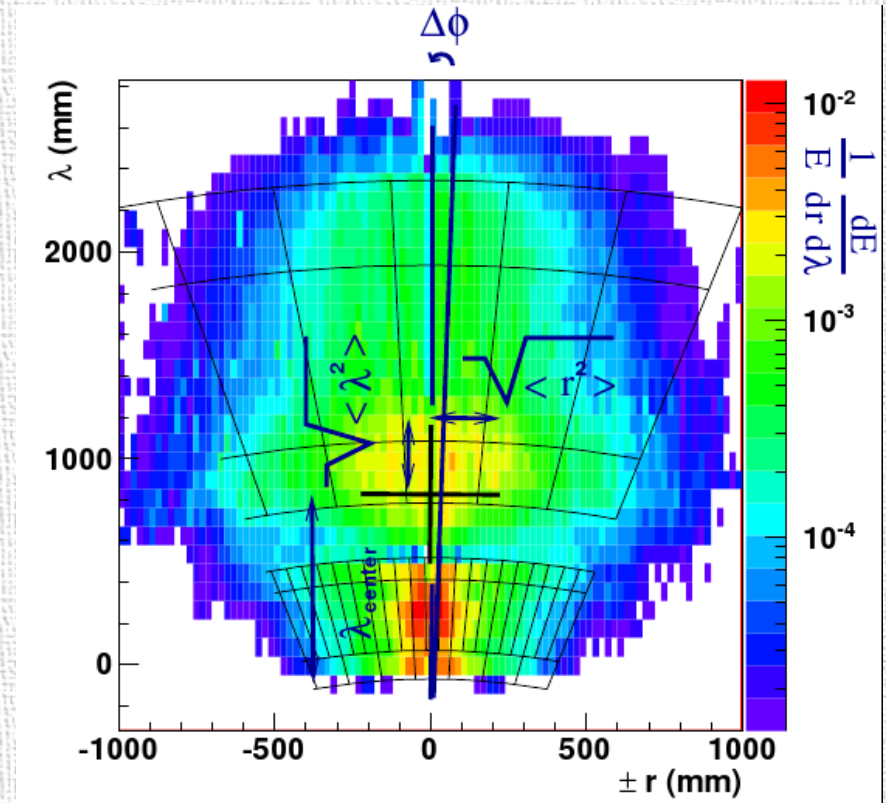
Cluster moments

n_{th} cluster moment of x defined as

$$\langle x^n \rangle = \frac{1}{\sum_i E} \cdot \sum_i E_i x_i^n \quad \text{looping over cells } i$$

Cluster moments used in the local hadronic calibration

- First moment of energy density
- Shower depth λ_{center}
 - distance between shower center and calorimeter front face
- Shower length
 - sqrt() of second moment of λ (λ is distance of cell from shower center)
- Shower width
 - sqrt() of second moment of r , where r is distance of cell from shower axis
- Isolation moment
 - Fraction of cells on the outer cluster perimeter which are not included in any other cluster

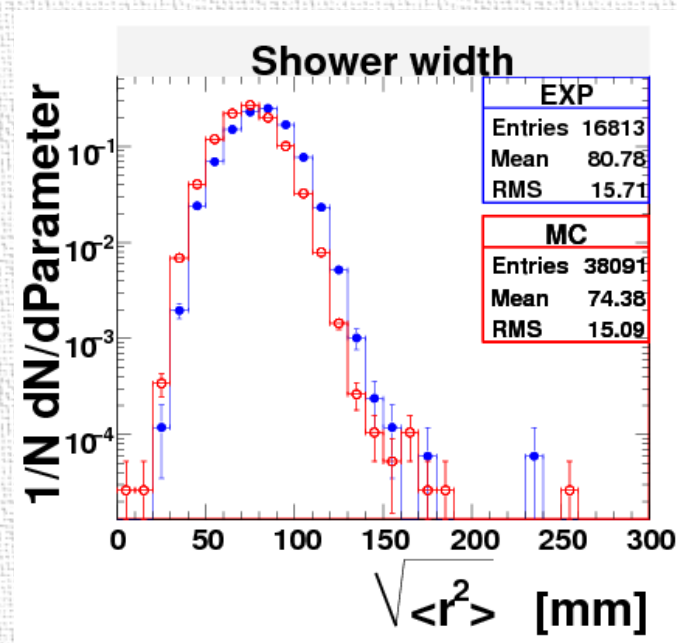
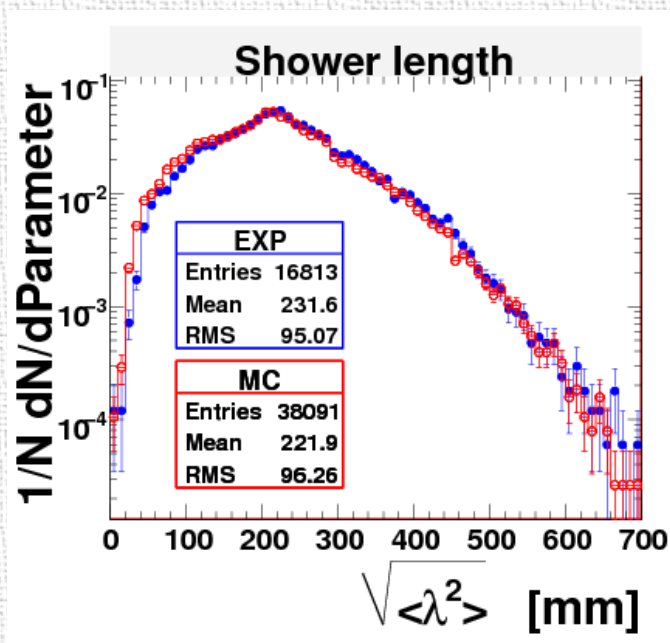
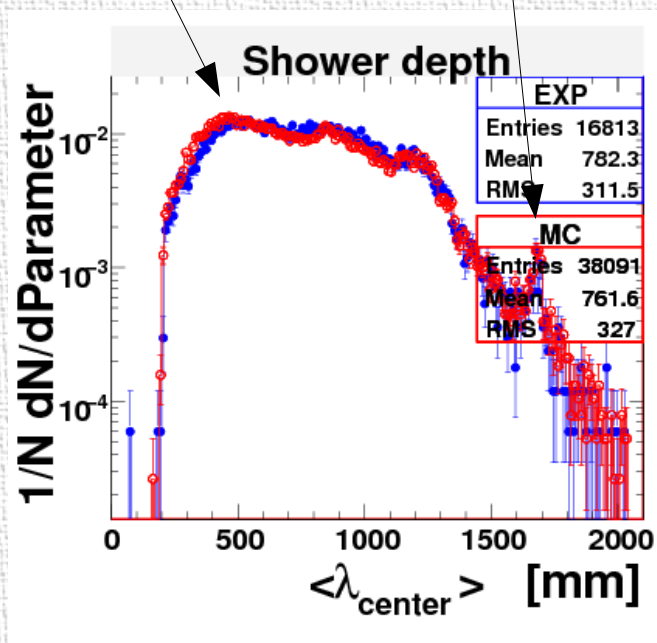


Cluster moments for the endcap region

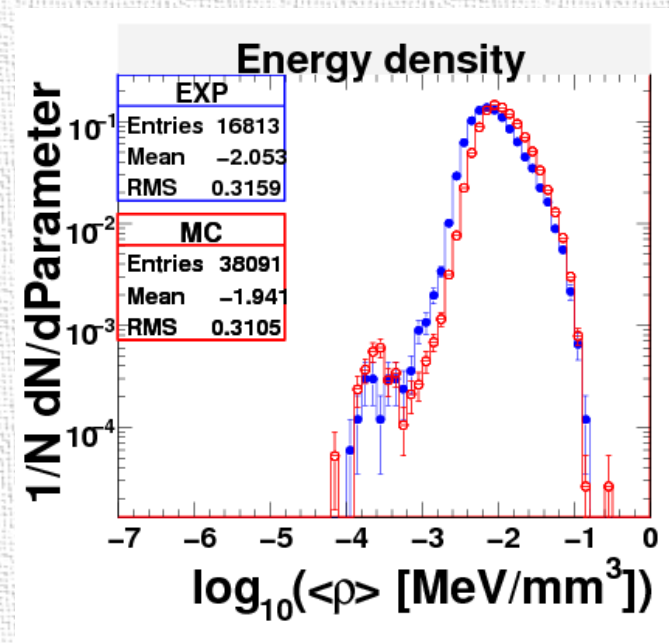
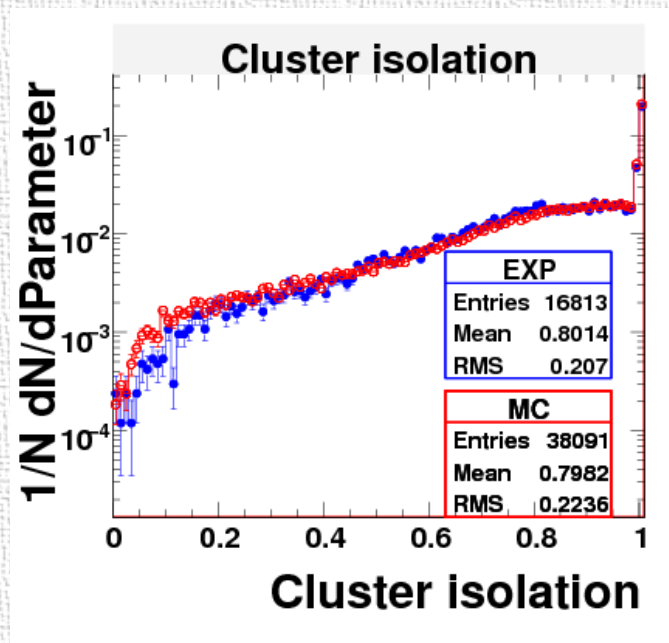
- Comparison of shower depth (left), shower length (center) and shower width (right) in Monte-Carlo and data
 - 200 GeV pions
 - shower starts slightly earlier in MC

Most of energy is deposited in the e.m. calorimeter

Shower is nearly completely contained in the had. calorimeter

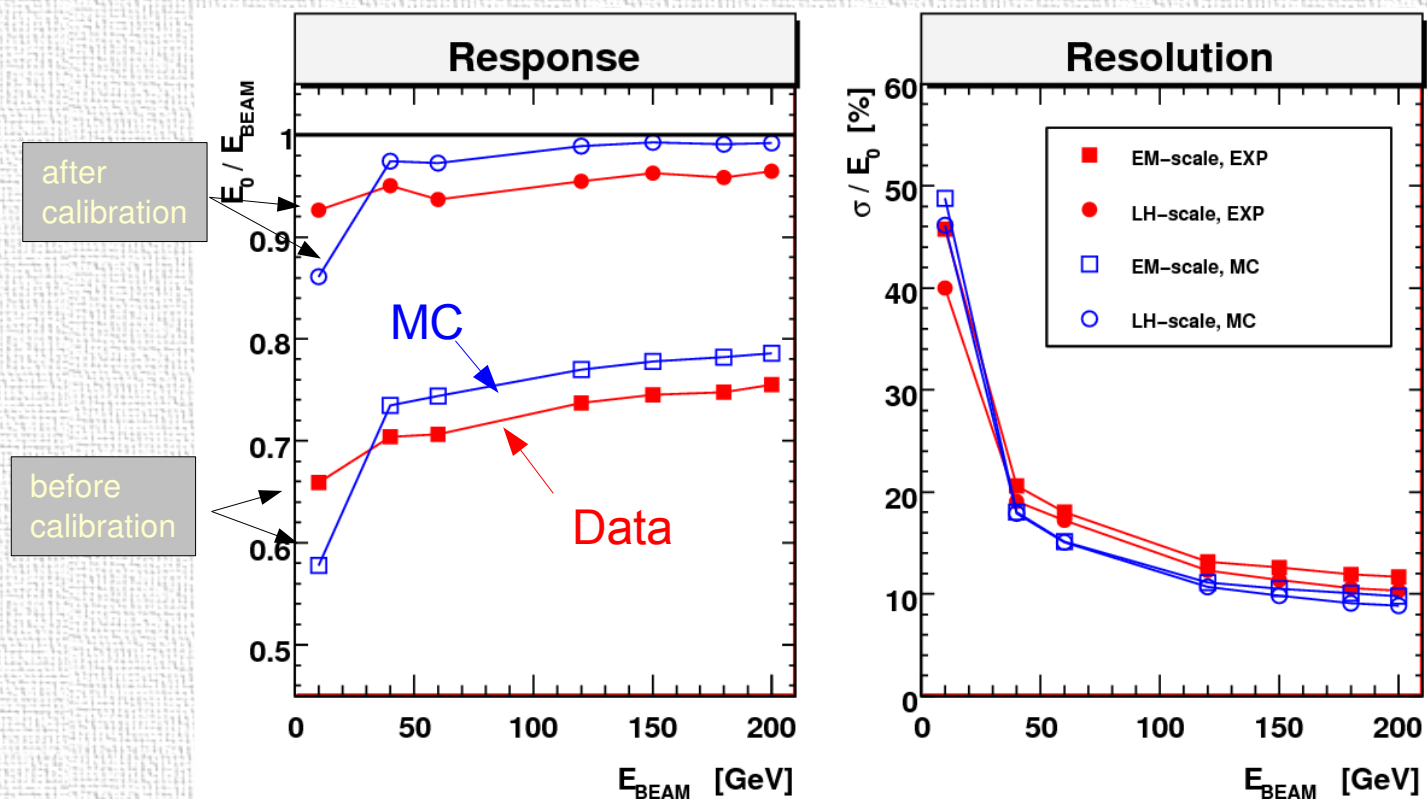


Cluster moments for the endcap region



- Comparison of degree of cluster isolation (left) and average cluster energy density (right) in Monte-Carlo and data.
 - Slightly denser shower in Monte-Carlo

Linearity and resolution (preliminary) for pions



- Plot shows the linearity (left) and the resolution (right) for $10 \leq \pi^- \leq 200$ GeV, data and MC, in endcap region (Point D)
 - ➔ Response in Monte-Carlo at e.m. scale level for charged pions is 5% higher, than in the data (this is a bias introduced by QGSP_BERT list). After calibration same difference remains.
 - ➔ In Monte-Carlo after calibration linearity recovered at 2% to 5% level for pion energies larger, than 20 GeV. There is no big improvement in resolution – testbeam specific constants have to be used instead of ATLAS ones (in particular for dead material corrections).

Conclusion

- Local hadronic calibration procedure is a simulation-based technique used in ATLAS to calibrate topological clusters from e.m. scale to particle level
- The validation of this procedure is in progress using ATLAS LAr combined testbeam data (2004)
 - Hadronic calibration constants based on ATLAS geometry have been used
- For pions Monte-Carlo **Geant4_9.2_QGSP_BERT** does not describe data perfectly
 - We see a standard feature of QGSP_BERT – slightly denser shower, which starts earlier in calo
 - Pion energy response is described within 5%
 - Simulation underestimates data resolution by 20%
 - Longitudinal and lateral shapes of the shower are described quite well
 - Reasonable good description of response for electrons in crack scans
 - Limited acceptance makes results very sensitive to a proper shower description in MC
- Local hadronic calibration is able to restore linearity at 2% for Monte-Carlo
 - e.m. scale for hadrons has to be tuned
- Relative energy resolution is expected to improve by 20%, while it remains the same
 - New testbeam specific set of correction coefficients has to be applied (to account for limited acceptance, and different dead material)

Backup slides

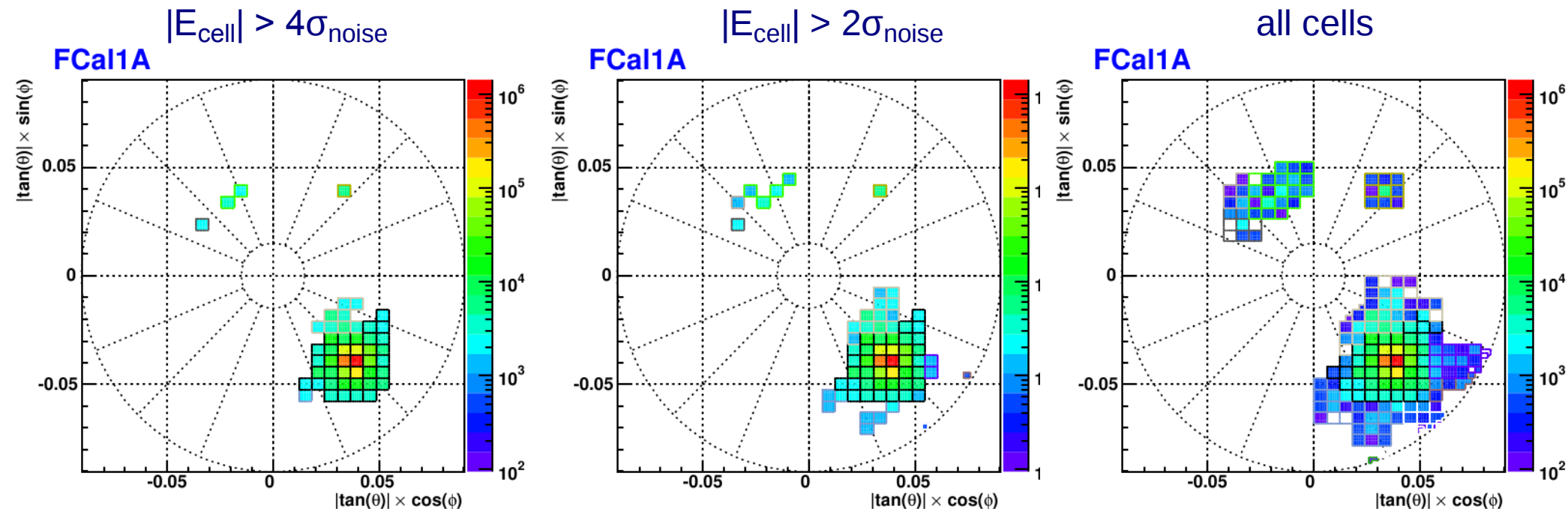
Topological clusters

Cluster making algorithm

- form cluster around seed cells with $|E_{\text{cell}}| > S \cdot \sigma_{\text{noise}}$, $S=4$
- expand in 3D, add neighbours with $|E_{\text{cell}}| > N \cdot \sigma_{\text{noise}}$, $N=2$
- add perimeter cells with $|E_{\text{cell}}| > P \cdot \sigma_{\text{noise}}$, $P=0$
- Seed/Neighbour/Perimeter formula = 4/2/0 good for combined beam tests

Cluster splitting algorithm

- split clusters around local maxima with maxima threshold $E > 500\text{MeV}$
- one cell can share energy between two clusters
- aim is to have one cluster per isolated e^\pm, μ, γ , currently $N_{\text{particle}}/N_{\text{clusters}} = 1.6$ in jet context



Classification

To identify EM and non-EM parts of the shower

Uses following shower shape variables (so-called cluster moments):

- λ_{center} cluster barycenter depth in calorimeter
- $\langle \rho_{\text{cell}} \rangle$ average cell energy density

High average cell energy density and small calorimeter cluster depth denotes EM nature of the cluster.

4-dimensional phase space for clusters in

$$|\eta|, E_{\text{cluster}}, \log_{10}(\lambda_{\text{center}}), \log_{10}(\langle \rho_{\text{cell}} \rangle)$$

is binned and filled with simulated pions in the energy range

$$200\text{MeV} < E_{\text{cluster}} < 2\text{TeV}$$

Fraction of neutral and charged pions in given phase-space bin i is used to calculate weight:

$$w_i = n_{\pi^0}^i / (n_{\pi^0}^i + 2 n_{\pi^\pm}^i)$$

At reconstruction stage cluster will be treated as electromagnetic if lookup value for $w > 0.5$ at a given cluster phase-space point.

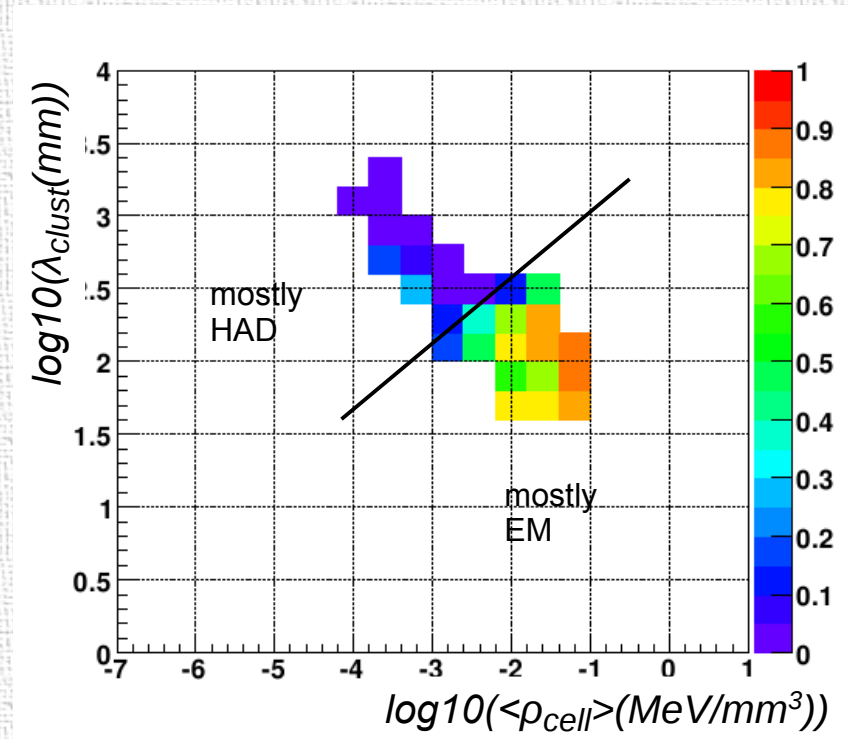


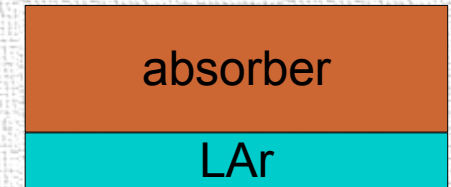
Table of probability for cluster to be EM
 $2.0 < |\eta| < 2.2$, $4\text{GeV} \leq E_{\text{cluster}} < 16\text{GeV}$

Weighting

Cell weights are derived from true energy deposits in LAr+Absorber (calibration hits) and accounts for invisible energy.

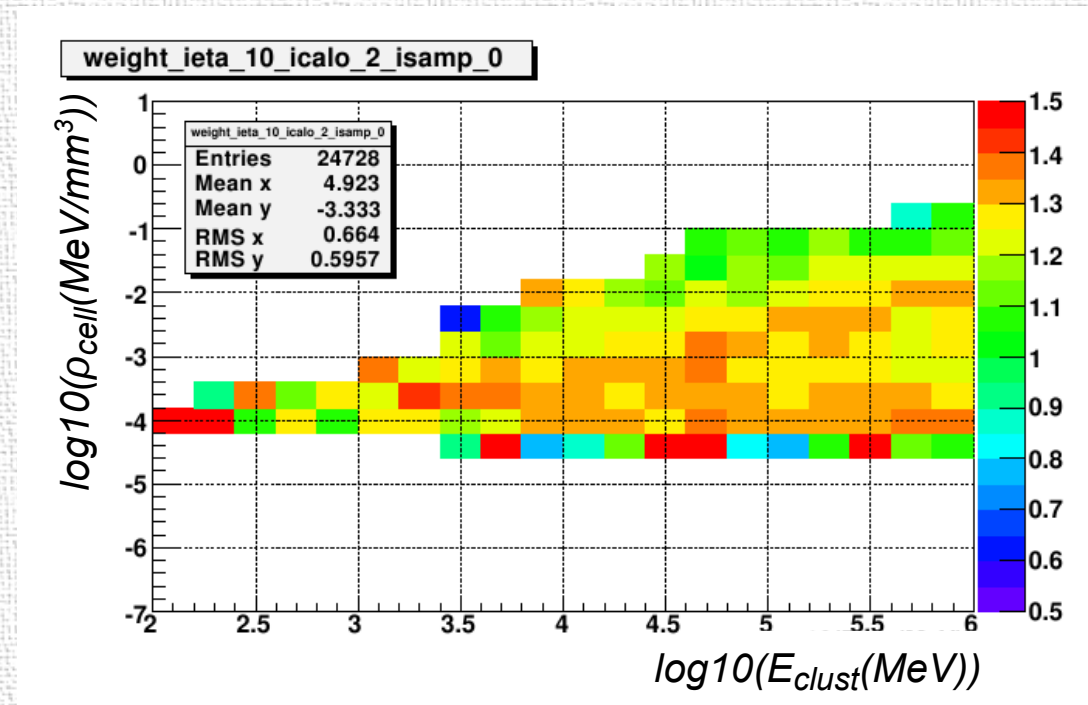
$$E'_{cell} = w \cdot E_{cell},$$

$$w = \left\langle \underbrace{\left(E_{cell}^{Em} + E_{cell}^{nonEm_{vis}} + E_{cell}^{nonEm_{invis}} + E_{cell}^{escaped} \right)}_{\text{calibration hits}} \right\rangle / \underbrace{\left\langle E_{cell}^{reco} \right\rangle}_{\text{cell signal at em scale (with noise and HV correction)}}$$



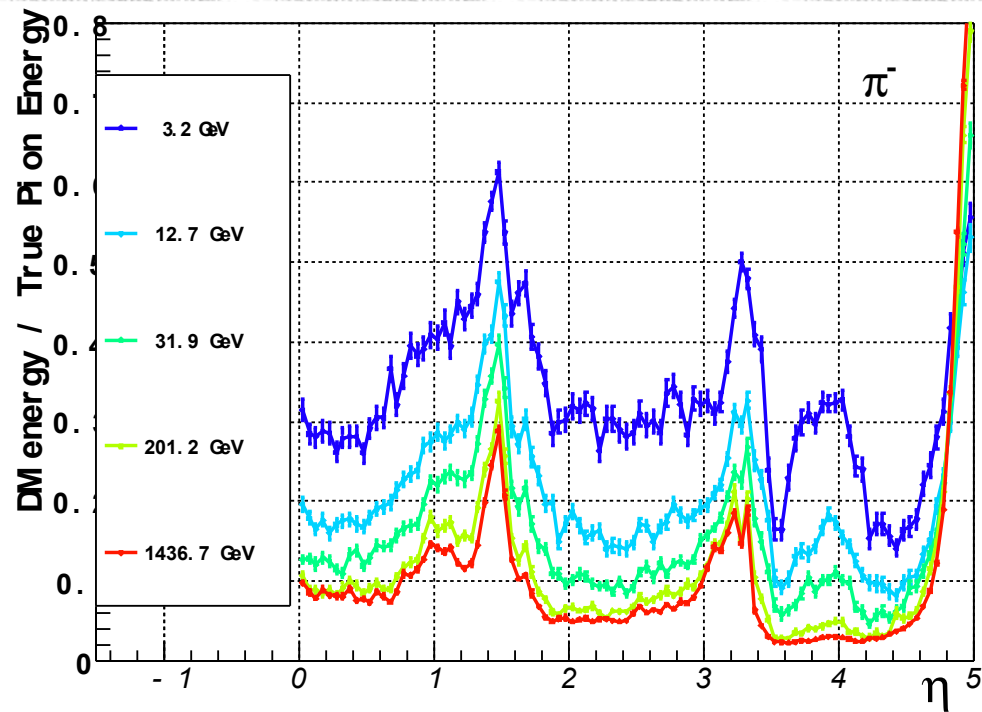
Weights are kept as a function of cluster energy $E_{cluster}$ and cell energy density $\langle \rho_{cell} \rangle$, for different η regions and longitudinal sampling.

Weights are applied only to the clusters classified as hadronic.



Hadronic cell weight table for $2.0 < |\eta| < 2.2$, HEC layer 1

Dead material correction



Dead material (DM) correction accounts for energy deposited outside of active calorimeter volumes.

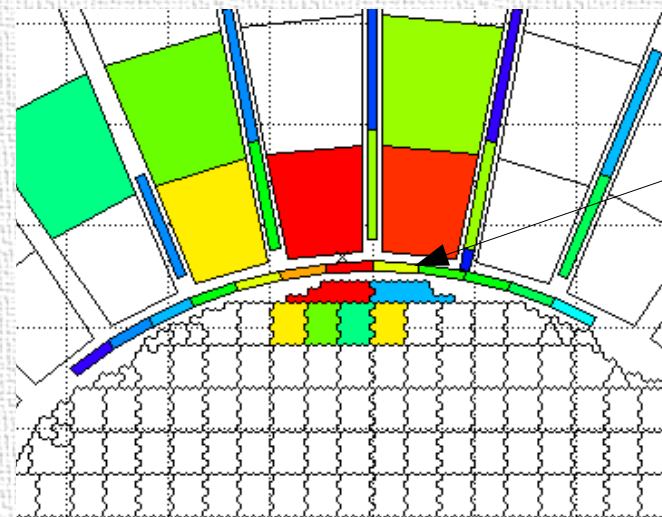
← Average ratio of DM energy to the beam energy versus $|\eta|$ for charged pions at different energies.

Energy losses outside of calorimeter cell volumes are stored in dead material calibration hits - virtual cells (70000 total) with 0.1×0.1 typical granularity.

Correction is derived for each DM region separately using correlation of DM energy losses (MC) and cluster quantities calculated at electromagnetic scale.

example:
energy lost between EMEC and HEC calorimeters is parametrized as a function

$$\sqrt{E_{\text{EMEC}} * E_{\text{HEC}}}$$



dead material calibration hit in the crack between HEC and FCAL

Energy in calorimeters in the endcap region (point D)

